

Mutational analysis of histidine residues in the human proton-coupled amino acid transporter PAT1

Linda Metzner^a, Kristin Natho^a, Katja Zebisch^a, Madlen Dorn^{a,b}, Eva Bosse-Doenecke^b,
Vadivel Ganapathy^c, Matthias Brandsch^{a,*}

^a Membrane Transport Group, Biozentrum, Martin-Luther-University Halle-Wittenberg, D-06120 Halle, Germany

^b Institute of Biochemistry/Biotechnology, Faculty of Sciences I, Martin-Luther-University Halle-Wittenberg, D-06120 Halle, Germany

^c Department of Biochemistry and Molecular Biology, Medical College of Georgia, Augusta, GA 30912-2100, USA

Received 5 September 2007; received in revised form 27 December 2007; accepted 28 December 2007

Available online 12 January 2008

Abstract

The proton-coupled amino acid transporter 1 (PAT1) represents a major route by which small neutral amino acids are absorbed after intestinal protein digestion. The system also serves as a novel route for oral drug delivery. Having shown that H^+ affects affinity constants but not maximal velocity of transport, we investigated which histidine residues are obligatory for PAT1 function. Three histidine residues are conserved among the H^+ -coupled amino acid transporters PAT1 to 4 from different animal species. We individually mutated each of these histidine residues and compared the catalytic function of the mutants with that of the wild type transporter after expression in HRPE cells. His-55 was found to be essential for the catalytic activity of hPAT1 because the corresponding mutants H55A, H55N and H55E had no detectable L-proline transport activity. His-93 and His-135 are less important for transport function since H93N and H135N mutations did not impair transport function. The loss of transport function of His-55 mutants was not due to alterations in protein expression as shown both by cell surface biotinylation immunoblot analyses and by confocal microscopy. We conclude that His-55 might be responsible for binding and translocation of H^+ in the course of cellular amino acid uptake by PAT1.

© 2008 Elsevier B.V. All rights reserved.

Keywords: Amino acid transport; PAT1; Histidine residues; Site directed mutagenesis; Drug delivery; Proline

1. Introduction

The proton-coupled amino acid transporter 1 (PAT1) was originally identified as the rat brain lysosomal amino acid transport system LYAAT1, which belongs to the amino acid/auxin permease system [1]. Subsequently, the cDNA encoding

the transporter was isolated from mouse intestine [2] and human Caco-2 cells [3]. The transporter was assigned to the solute carrier (SLC) family 36 as SLC36A1 [2,3]. hPAT1 is identical to the H^+ -stimulated amino acid transporter that has been described functionally in Caco-2 cells in previous reports [4,5]. Expression of the PAT1 mRNA was detected not only in brain and small intestine but also in liver, colon, lung, spleen and placenta [2,3,6]. Prototype PAT1 substrates are L-proline, glycine, β -alanine, γ -aminobutyric acid (GABA) and α -(methylamino)-isobutyric acid (MeAIB) [2–4,6–9].

PAT1-mediated transport depends on an inwardly directed H^+ gradient. H^+ is co-transported with the substrates into the cell [6,9]. The binding occurs in an ordered mechanism where H^+ binds first, followed by the amino acid [10]. Transporters which are energized by a transmembrane H^+ gradient possess specific histidine residues that are critical for their catalytic activity. The uniqueness of the histidine residue resides in the intraprotein pK_a

Abbreviations: CHDP, *cis*-4-hydroxy-D-proline; CHLP, *cis*-4-hydroxy-L-proline; DAPI, 4',6-diamidino-2-phenylindole dihydrochloride; DEPC, diethylpyrocarbonate; GABA, γ -aminobutyric acid; HA, hemagglutinin; HRPE, human retinal pigment epithelium; IU, infectious units; LACA, L-azetidine-2-carboxylic acid; MeAIB, α -(methylamino)isobutyric acid; MVA, modified vaccinia virus Ankara; PAT1, proton-coupled amino acid transporter 1; PEPT1, peptide transporter 1; TMD, transmembrane domain

* Corresponding author. Biozentrum of the Martin-Luther-University Halle-Wittenberg, Membrane Transport Group, Weinbergweg 22, D-06120 Halle, Germany. Tel.: +49 345 552 1630; fax: +49 345 552 7258.

E-mail address: matthias.brandsch@biozentrum.uni-halle.de (M. Brandsch).

value of 6.7–7.1 for the imidazole group of its side chain which is very close to the physiological pH. This characteristic renders the histidine residues capable of easily accepting and releasing H^+ under physiological conditions. Thus, histidine is the most likely amino acid residue involved in H^+ binding and translocation in H^+ -coupled transport systems such as the peptide transporters PEPT1 and PEPT2, the divalent metal transporter DMT1, the folate transporter PCFT, the organic anion transporting polypeptide OATP2B1, the excitatory amino acid carrier EAAC1, and others [for review see 11]. The *Escherichia coli* Lac permease, a prototypical H^+ -coupled transport system has been extensively studied with regard to the role of critical histidine residues in the binding and translocation of the cotransported H^+ [12]. Diethylpyrocarbonate (DEPC), known to block the H^+ acceptor/donor function of histidine residues of proteins by producing *N*-carboxyhistidine residues, increased the apparent K_m of H^+ -coupled lactate and proline transport in *E. coli* membrane vesicles with no change in V_{max} [12]. For the mammalian H^+ -coupled di- and tripeptide transporter PEPT1, we have shown that both H^+ and treatment with DEPC modulate the maximal velocity of peptide transport [13]. Subsequently, in site-directed mutagenesis studies it was shown specifically that His-57 is essential for the catalytic activity of human PEPT1 [14]. Said and Mohammadkhani [15] observed a mixed type inhibitory effect of DEPC on intestinal carrier-mediated folate transport. The monocarboxylate transporter MCT1 is also a H^+ -coupled transporter and its transport function is inhibited by DEPC; however, it appears that histidine residues are not involved in this process because the inhibition caused by DEPC is not reversed by hydroxylamine [16]. Later studies by Rahman et al. have suggested that Asp-302 may be involved in H^+ monocarboxylate cotransport via MCT1 [17]. For hPAT1, we have demonstrated very recently that H^+ and DEPC-treatment strongly affect the affinity of the carrier protein for several substrates but not the maximal velocity of L-proline transport [18]. The present investigation using site-directed mutagenesis was performed to identify the histidine residues that are critical for the catalytic activity of PAT1. The hPAT1 protein consists of 476 amino acid residues, 10 of them being histidine residues. Mutational analyses of PAT1 or the other 3 members of the SLC36 transporter family [19] have not yet been performed. The results of this investigation demonstrate that His-55 is obligatory for transport in hPAT1.

2. Materials and methods

2.1. Materials

L-[3H]Proline (specific radioactivity 49 Ci/mmol) was obtained from Amersham Biosciences (Little Chalfont, UK). Chemical reagents, the rabbit-anti-HA-Tag antibody and the β -tubulin III antibody were from Sigma (Taufkirchen, Germany). The chicken anti-hPAT1 antibody was raised against the synthetic peptide SSTDVSPEESPSEGL by Davids Biotechnology GmbH (Regensburg, Germany). Cell culture reagents and the secondary fluorophor-conjugated antibody AlexaFluor[®]488 goat anti-rabbit IgG was purchased from Invitrogen (Karlsruhe, Germany). The secondary anti-chicken and anti-rabbit horseradish peroxidase conjugated antibodies were obtained from Santa Cruz Biotechnology, Inc. (Heidelberg, Germany). The recombinant modified vaccinia virus Ankara was provided by the GSF-Institute for Molecular Virology (Munich, Germany).

2.2. Site-directed mutagenesis

The QuickChange[®] Site-Directed Mutagenesis Kit (Qiagen, Hilden, Germany) was used to mutate the three selected histidine codons (CAC) in hPAT1 or HA-Tagged hPAT1 to an alanine codon (GCC) or an asparagine codon (AAC), respectively, according to the manufacturer's protocol. The primers used to mutate these histidine residues in the plasmid pSPORT1-hPAT1 were as follows: (H55A) 5'CCAGACCTTGATCGCCCTGTAAAAGGAAACATTG3', (H55N) 5'GTTCCAGACCTTAATCAACCTGTAAAAGGCAAC3', (H93A) 5'GGTTCAGACCCCTGATCGAGCTGTAAAAGGC3', (H93A) 5'CATCGTGGCCGTGGCCTGCATGGGTATCCTG3', (H93N) 5'GCATCGTGGCCGTGA[~]ACTGCATGGGTATCCTGG3', (H135A) 5'TCCTGGCTCCGGAACGCCGCACACTGGGGAAGA3', (H135N) 5'TCCTGGCTCCGGAACA[~]ACGCACACTGGGGAAGA3'. The QIAprep[®] Spin Miniprep Kit (Qiagen, Hilden, Germany) was used to isolate the plasmid DNA. The specific mutations were verified by sequencing (MWG Biotech AG, Ebersberg, Germany). For this, the primers 5'TAATACGACTCACTATAGGG'3 and 5'GGTGATTCTGACG CCTAC3' were used.

2.3. Construction of HA-Tagged hPAT1

The DNA sequence encoding the HA-epitope was fused to the N-terminus of the hPAT1 plasmid-cDNA by PCR. Oligo GATTGAATTCATGTATCCGTACGATGTTCTCTGACTATGCGGGTATGTCCACGCAGAGA was the 5' primer, oligo GTTAGCGGCCGCTATATGAAGGCACAG the 3' primer, and pSPORT1-hPAT1 the template. The PCR product was cut with restriction endonucleases EcoR I and Not I and inserted into the EcoR I/Not I digested pSPORT1 vector. The insertion was verified by DNA sequencing and restriction digestion by the endonucleases EcoR I and Not I.

2.4. Cell culture

Human retinal pigment epithelial (HRPE) cells (passages 8–40), maintained in 75 cm² flasks (Sarstedt, Nümbrecht, Germany), were cultured in D-MEM/F12 supplemented with 10% fetal bovine serum (Biobrom, Berlin, Germany) and 1% penicillin/streptomycin (Invitrogen, Karlsruhe, Germany). Cells were released by rinsing with PBS and trypsinization and subcultured in 75 cm² flasks, 6-well or 24-well plates (Sarstedt, Nümbrecht, Germany) at densities of 6×10^6 per flask and 1.6×10^6 or 0.5×10^6 per well.

2.5. Functional expression of hPAT1 or HA-hPAT1 in mammalian cells

HRPE cells were transiently transfected using the modified vaccinia virus Ankara (MVA) encoding T7 RNA polymerase [3,20]. Amplification, purification and titration of recombinant MVA to determine the amount of infectious units per ml were performed in BHK-21 cells according to the protocol reviewed by Staib et al. [21]. Subconfluent HRPE cells grown in 75 cm² flasks or in 6-well and 24-well plates were infected 22–24 h after seeding with the recombinant MVA (50 IU/cell). At this stage the cell number that is referred to in results was determined from control wells at a CASY[®]TT cell counter (Schärfe System GmbH, Reutlingen, Germany). Next, cells were transfected with the plasmid DNA (hPAT1, HA-hPAT1, mutant, empty vector pSPORT1) using Nanofectin[®] according to manufacturers protocol (PAA Laboratories, Cölbe, Germany). The interaction of T7 RNA polymerase with the T7 promoter located on the expression plasmids results in the overexpression of the transporter proteins in the cells. To minimize toxic effects, medium replacement was performed 3 h after transfection. 21 h post-transfection, uptake measurements, biotinylation, or immunofluorescence experiments were initiated.

2.6. Uptake measurements in hPAT1 cDNA or HA-hPAT1 cDNA transfected cells

Before the uptake experiment, cells were washed with the respective uptake buffer. Uptake was started by incubating the cells with uptake buffer at different pH values containing 25 mM Mes/Tris or HEPES/Tris, 140 mM NaCl, 5.4 mM KCl, 1.8 mM CaCl₂, 0.8 mM MgSO₄, 5 mM glucose and 20 nM L-[3H]proline at room temperature. In some experiments sodium chloride was replaced by

choline chloride (140 mM). After the respective time periods, the incubation was stopped by rinsing the monolayers four times with ice cold uptake buffer. Samples were prepared for liquid scintillation spectrometry (Tri-Carb 2100TR, Packard Instrument Company, Meriden, USA) by suspending the cells in 0.5 ml lysis buffer (0.2 M NaOH, 1% SDS) and 2.8 ml scintillation cocktail. Protein was determined according to the method of Bradford. On average, the protein content of a well in a 24-well plate was 0.05 mg.

2.7. Cell surface biotinylation

22–24 h after seeding HRPE cells in 75 cm² flasks (6×10^6 cells per flask), cells were transfected with the empty vector pSPORT1 alone or the construct containing the full-length hPAT1, the HA-hPAT1 or the respective mutants cDNA. Cell-surface-expression levels were examined 21 h after transfection using the membrane-impermeant EZ-Link[®] Sulfo-NHS-SS-Biotin (Pierce, Rockford, USA). After removing the medium, cells were washed twice with ice cold PBS containing 0.1 mM CaCl₂ and 0.1 mM MgCl₂ (PBS-Ca²⁺/Mg²⁺) and then incubated for 20 min at 4 °C on a shaker with EZ-Link[®] Sulfo-NHS-SS-Biotin dissolved in ice-cold PBS-Ca²⁺/Mg²⁺ (1 mg/ml). Unbound biotin was quenched after washing twice with PBS-Ca²⁺/Mg²⁺ by incubating the cells with PBS-Ca²⁺/Mg²⁺ containing 100 mM glycine for 20–30 min at 4 °C on a shaker. Cells were then washed three times with PBS-Ca²⁺/Mg²⁺ and scraped into this buffer, transferred into a 15 ml tube and centrifuged (400 g, 15 min). The pellet was resuspended in lysis buffer (150 mM NaCl, 1 mM EDTA, 100 mM Tris-HCl, 1% Triton-X-100, 1% sodium deoxy cholate, 0.1% sodium dodecyl sulfate), containing protease inhibitors (Roche Diagnostics GmbH, Mannheim, Germany), sonicated five times and incubated in this buffer for 30 min on ice to assure total lysis. After centrifugation (14 600 g, 4 °C, 20 min), protein concentration of lysates was determined. Protein (150–200 µg) was added to 100 µl NeutrAvidin[®] beads (Pierce, Rockford, USA), incubated for 1 h at room temperature on a shaker and then centrifuged (14 600 g, 15 min) to batch-extract biotinylated proteins. After washing the beads four times with lysis buffer and centrifugation (14 600 g, 5 min), bound membrane proteins were released by incubation with 50 µl of sample buffer (50 mM Tris-HCl, pH 6.8, 2 mM EDTA, 4% SDS, 8 M urea, 3.5% 2-mercaptoethanol, 0.001% bromophenol blue) for 30 min on a shaker.

2.8. Western blot analyses

Lysates and cell surface proteins were separated by SDS-PAGE in 12% gels, transferred to nitrocellulose membranes (Roth, Karlsruhe, Germany) and then subjected to Western blot analysis. After blotting and blocking, the membranes were incubated with the primary antibody (chicken anti-hPAT1 or rabbit anti-HA-Tag) in TBT buffer (10 mM Tris, 150 mM NaCl, 0.2% Tween, pH 7.4) containing 5% nonfat dry milk overnight at 4 °C on a shaker. The second antibody (anti-chicken horseradish peroxidase-conjugated or anti-rabbit horseradish peroxidase-conjugated) was added after washing the membrane with TBT buffer and the membrane was incubated for 1 h at 4 °C on a shaker. Signals were detected using an X-ray film (Amersham, München, Germany).

2.9. Confocal laser scanning microscopy

Transfected HRPE cells were grown on coverslips in 6-well plates. Cells were fixed and permeabilized with ice cold PBS containing 4% paraformaldehyde and 0.05% Triton-X-100 for 20 min. Excess of paraformaldehyde was removed by incubation with 0.1 mM NH₄Cl. After blocking with 5% bovine serum albumin in PBS, cells were incubated for 2 h with the primary antibody (rabbit anti-HA-Tag) diluted 1:2000 in 5% bovine serum albumin in PBS. The second antibody (anti-rabbit AlexaFluor[®] 488) was used in a 1:500 dilution with an incubation time of 1 h. Nuclei were stained with DAPI (4',6-diamidino-2-phenylindole dihydrochloride; 1:100 in PBS). Coverslips were mounted in CitiFluor[®] (Plano, Wetzlar, Germany) and samples were examined with a Nikon ECLIPSE TE2000.

2.10. DEPC experiments

HRPE cells expressing hPAT1 or HA-hPAT1 mutants were washed twice with buffer pH 7.5 (25 mM HEPES/Tris; containing 140 mM NaCl, 5.4 mM

KCl, 1.8 mM CaCl₂, 0.8 mM MgSO₄, 5 mM glucose) and then incubated with DEPC or ethanol as vehicle in buffer for 0–10 min at room temperature. The DEPC stock solutions were prepared in ethanol before the experiment and freshly added to each well at a final concentration of 0–1.5 mM (vehicle: 0.2%). After the desired DEPC-incubation time, cells were washed twice and incubated with uptake buffer pH 6.0 containing L-[H]proline (20 nM) with or without increasing concentrations of unlabeled L-proline (0–10 mM).

2.11. Calculations and statistics

All data are given as the mean \pm S.E. of three to six independent experiments. The Michaelis–Menten constant (K_m) and the maximal velocity of transport (V_{max}) were calculated by nonlinear regression of the Michaelis–Menten plot (Sigma Plot 8.0, SPSS Inc., Chicago, USA). Statistical analysis was done by the non-parametric two-tailed *U*-test and a *P* value of less than 0.05 was considered statistically significant.

3. Results and Discussion

3.1. Conserved histidine residues in the PAT-family

The solute carrier gene family SLC36 contains the genes coding for the H⁺-coupled amino acid transporters PAT1 to 4 [2,9,19]. Mammalian PAT1 has been characterized on a molecular level in mouse, rat, rabbit, chimpanzee and human. The sequence of PAT2 is known from mouse, rat and human. Both PAT1 and PAT2 have been analyzed with regard to function, localization and specificity whereas PAT3 and 4 are still orphan transporters. The mRNA of PAT1 occurs ubiquitously but is slightly more abundant in brain, small intestine, colon, kidney, lung and spleen [2,3]. PAT2-mRNA has been detected in lung, heart, kidney, muscle, testis, spleen and adrenal gland [2]. The four SLC36 proteins consist of 470 to 504 amino acid residues with molecular weights of 53.28 kDa (hPAT1), 53.22 kDa (hPAT2), 51.76 kDa (hPAT3) and 56.16 kDa (hPAT4) and exhibit at least 48% identity to each other. In Fig. 1, a partial alignment of human PAT1 to 4 and the respective PAT1 homologs in mouse, rat and rabbit are shown. The human PAT1 protein consists of 476 amino acid residues, 10 of them being histidine residues. The histidine residues His-55, His-93 and His-135 in hPAT1 are conserved both among PAT1 to 4 and the four species. Assuming the 11 TMD topology for hPAT1, His-55 and His-93 are located in the first and second transmembrane domain and His-135 is located in the first intracellular loop (Fig. 1).

3.2. Functional characterization of hPAT1

Employing the vaccinia virus (MVA) expression method, HRPE cells were used as a mammalian system for heterologous expression of hPAT1. Cells were transiently transfected with the cDNA of hPAT1 or the empty vector pSPORT1. Uptake of L-[³H]proline at pH 6.0 in HRPE cells expressing hPAT1 was linear for up to 20 min (data not shown). All further experiments were performed using a 10 min incubation time. L-[³H]Proline transport was first measured in uptake buffer at pH values varying from 5.0 to 8.5. As shown in Fig. 2 (left inset), L-[³H]proline uptake was strongly stimulated by an inwardly directed H⁺ gradient. At pH 7.5 and 8.5, the hPAT1-specific uptake was barely detectable. Subsequent uptake experiments were

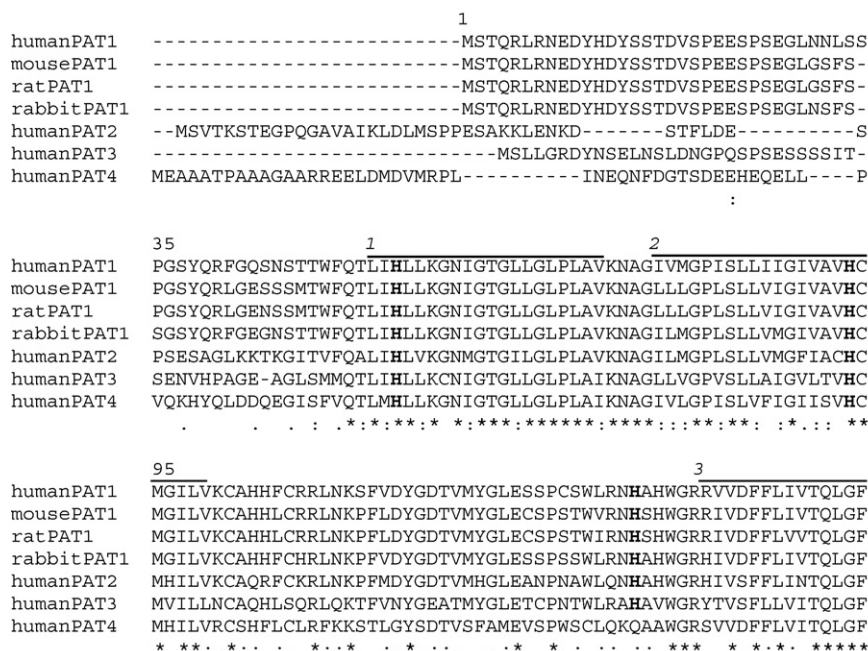


Fig. 1. Partial multiple sequence alignment of PAT1 proteins from human, mouse, rat, rabbit PAT1 and human PAT2 to PAT4 proteins. The alignment was performed using the Toffee program. (www.ch.embnet.org/software/TOffee.html). (*) Identical, (.) conserved and (:) semi-conserved residues and putative transmembrane helices are designated.

performed at an extracellular pH of 6.0. To verify that hPAT1 mediated transport is Na^+ independent as it has been shown by others [2–4,6,7,9], L-[^3H]proline uptake in HRPE cells was measured in the absence and presence of Na^+ (Fig. 2, right inset). The hPAT1-specific L-[^3H]proline uptake in the absence of Na^+ (260 ± 33 fmol/10 min per 400 000 cells) was not significantly different from the uptake in the presence of Na^+ (230 ± 34 fmol/10 min per 400 000 cells). Further experiments were performed in the presence of Na^+ . Under these conditions, i.e. using a 10 min incubation at pH 6.0 in the presence of Na^+ , uptake of L-[^3H]proline in hPAT1 cDNA-transfected cells was about 10 to 20 fold higher than uptake in cells transfected with empty vector pSPORT1. Next, the substrate saturation kinetics of L-proline uptake into hPAT1 cDNA-transfected cells was determined by measuring uptake at increasing concentrations of L-proline (Fig. 2). L-Proline uptake was saturable with a Michaelis constant of 0.9 ± 0.1 mM and a maximal transport velocity of 8.6 ± 0.2 nmol/10 min per 400 000 cells. These transport properties correspond very well with previous data on PAT mediated amino acid transport obtained at Caco-2 cells, transfected mammalian cells or *Xenopus laevis* oocytes expressing PAT1 [2–4,6,7].

3.3. Generation and analysis of hPAT1 mutants

Six different mutants were generated by replacing the three conserved histidine residues by either alanine or asparagine. Two more mutants (double mutants) were obtained by converting both of the first two conserved histidine residues, His-55 and His-93, to alanine or asparagine, respectively. The mutants are designated as H55A, H55N, H93A, H93N, H55A/H93A, H55N/H93N, H135A and H135N. Alanine was chosen for mutation because of its very different properties compared to

histidine. Asparagine was selected for substitution to exclude as far as possible local structural perturbations because replacement of histidine with this amino acid would have minimal steric effect on the resultant mutant protein. L-[^3H]Proline uptake experiments were performed in non-transfected HRPE cells (NT) and HRPE cells transfected either with the empty vector (pSPORT1) or the construct containing the hPAT1 or the mutated cDNA. Compared to hPAT1, the mutants H55A, H55N, H93A and the double mutants H55A/H93A and H55N/H93N displayed a dramatic loss of uptake function (data not shown, see below). Uptake by H55A and H55N mutants was 10 or 22%, respectively, compared to control. With regard to His-93, it was observed that replacement with alanine reduced uptake activity by 78% whereas the conversion to asparagine reduced uptake by only 22%. Neither alanine nor asparagine binds H^+ but substitutions of histidine residues with asparagine may cause less structural perturbations than substitutions with alanine. There was no impact of a mutation of His-135. Both H135A and H135N mutants transport L-[^3H]proline at a rate near control value. To rule out a pH shift effect on proline uptake caused by the mutational changes, we measured uptake both at pH 6.0 and 7.5. At pH 7.5 all L-[^3H]proline uptake rates were at the same low level (~ 43 fmol/10 min per 400 000 cells) and almost identical in non-transfected and transfected cells. We concluded that mutants H55A, H55N, H93A, H55A/H93A and H55N/H93N but not mutants H93N, H135A and H135N lost their ability for H^+ -coupled L-[^3H]proline transport completely. It could be speculated that His-55 and perhaps His-93 but not His-135 might be critical for the H^+ stimulation of proline transport by hPAT1. However, this loss of function could also be explained by a decreased expression level of the respective mutant in the cell membranes of HRPE cells due to instability of mRNA, instability of protein, alterations in transporter

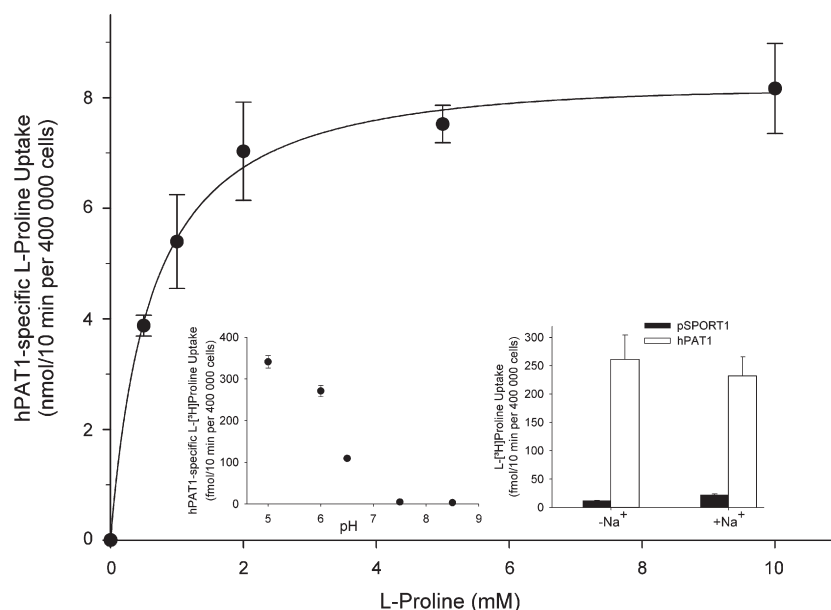


Fig. 2. hPAT1 cDNA-mediated L-proline uptake. Main figure: Substrate saturation kinetics of specific L-proline uptake. L-[³H]Proline uptake (20 nM; pH 6.0; 10 min, $n = 4$) was measured at varying concentrations of L-proline (0–10 mM) in cells transfected with either empty vector pSPORT1 as control or the construct containing the hPAT1 cDNA. Uptake in vector-transfected cells was subtracted from uptake in hPAT1-transfected cells to calculate hPAT1-specific uptake. Left inset: Influence of extracellular pH. L-[³H]Proline uptake (20 nM; 10 min) was determined at varying pH values, from 5.0 to 8.5. Data represent specific uptake of hPAT1 transfected cells. Right inset: Influence of Na⁺ on hPAT1 transport activity. L-[³H]Proline uptake was measured in cells transfected with either vector as control or the construct containing the hPAT1 cDNA at pH 6.0. Sodium chloride was isoosmotically replaced by choline chloride. Data are means \pm S.E.M., $n = 4$.

trafficking and many other effects. To study cell membrane expression of hPAT1 mutants, we initiated surface protein biotinylation and Western blot analyses. Immunoblot analyses with total cell lysate of Caco-2 cells were thought to serve as positive control for the specificity of the affinity-purified antibody raised against a 15-amino acid synthetic peptide sequence in hPAT1. Surprisingly, using this antibody hPAT1-like surface expression was detected in non-transfected HRPE cells (data not shown). From other studies we had independent evidence that the antibody recognizes full length hPAT1 in Western blot analyses quite specifically. But, even though there was no significant H⁺-dependent L-[³H]proline uptake in these cells (Fig. 2) we cannot rule out a very low but detectable expression of the protein. To circumvent this problem, we used the following strategy: A hemagglutinin (HA) epitope of 9 amino acid residues was fused to the N-terminus of hPAT1 cDNA. For this HA sequence, a very specific and high-affinity monoclonal antibody is available. This antibody could be used for the detection of HA-Tagged hPAT1, but first we had to investigate whether hPAT1 retained its transport properties after fusing the HA-Tag or whether this modification impairs transport function.

3.4. Functional expression of HA-hPAT1 and mutants

L-[³H]Proline uptake measurements were repeated as described using HRPE cells but this time transfected with HA-hPAT1 cDNA or empty vector pSPORT1. HA-hPAT1 showed identical transport function when compared with hPAT1. HA-hPAT1 specific L-proline uptake was Na⁺-independent but strongly stimulated in the presence of an inwardly directed H⁺ gradient. Uptake was saturable with a Michaelis constant of 1.5 ± 0.3 mM

and a maximal transport velocity of 11.9 ± 1.0 nmol/10 min per 400 000 cells (data not shown). To prove unequivocally that the transport function of HA-hPAT1 is similar to that of hPAT1, the substrate specificity of L-[³H]proline uptake in HRPE cells transfected with either hPAT1 cDNA or with HA-PAT1 cDNA was compared (Fig. 3). L-Proline and the derivatives (all 5 mM) CHLP, CHDP and LACA showed the same inhibitory potency in hPAT1 and HA-hPAT1 cDNA-transfected cells. The stronger

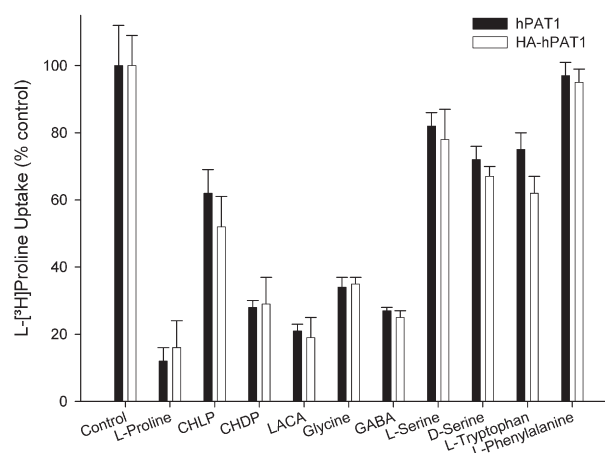


Fig. 3. Substrate specificity of hPAT1 and HA-hPAT1. Uptake of L-[³H]proline (20 nM) was measured in HRPE cells transfected with empty vector (pSPORT1) as control or the plasmid containing the wildtype hPAT1 or HA-PAT1 cDNA at pH 6 for 10 min in the presence of Na⁺ and unlabeled amino acids at a fixed concentration of 5 mM. L-[³H]Proline uptake measured in the absence of inhibitors (241 ± 26 fmol/10 min per 400 000 cells for hPAT1 and 209 ± 21 fmol/10 min per 400 000 cells for HA-hPAT1) was taken as 100%. Data represent the hPAT1 and HA-hPAT1 cDNA-specific uptake and are means \pm S.E.M., $n = 4$.

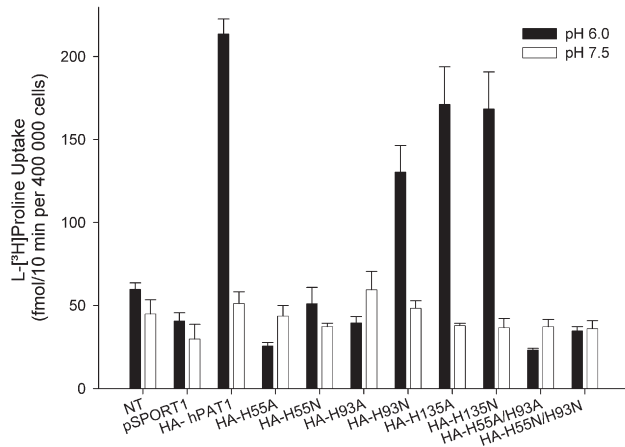


Fig. 4. Transport function of HA-hPAT1 and histidine mutants. L-[³H]proline uptake (20 nM; 10 min) was measured in non-transfected HRPE cells (NT) and in cells transfected with either empty vector pSPORT1 as control or the construct containing the HA-hPAT1 or mutant cDNA. Uptake measurements were performed in the presence (pH 6.0) and absence (pH 7.5) of an inward-directed H⁺ gradient. Data are means \pm S.E.M., $n = 4-6$.

inhibition of L-[³H]proline uptake by CHDP compared to CHLP confirms the preference of PAT1 for D-isomers of certain amino acids. Both the PAT1 substrates glycine, GABA, L-serine, D-serine [2,3,7] and the non-transported PAT1 inhibitor L-tryptophan [22] displayed identical inhibition rates. L-Phenylalanine is not transported and not recognized by the PAT1 protein. Accordingly, we found no interaction of L-phenylalanine with either hPAT1 or HA-hPAT1.

Next, exactly as the mutational modifications of hPAT1 cDNA were done, residues His-55, His-93 and His-135 were mutated in HA-hPAT1 cDNA to alanine or asparagine, respectively. These histidine mutants are designated as HA-H55A, HA-H55N, HA-H93A, HA-H93N, HA-H135A, HA-H135N and HA-H55A/H93A and HA-H55N/H93N. Functional analysis of HA-hPAT1 and mutants was performed using the L-[³H]proline uptake assay at cDNA-transfected HRPE cells. Fig. 4 shows the data for HA-hPAT1- and mutant-specific uptake. Mutations of His-55 to alanine or asparagine abolished L-[³H]proline uptake to the level of non-transfected cells as did mu-

tations to HA-H93A and double mutations HA-H55A/H93A and HA-H55N/H93N. Conversion of His-93 to asparagine reduced L-[³H]proline uptake by only about 36%. These results on HA-hPAT1-HRPE are virtually identical to those obtained at hPAT1-HRPE. We also mutated HA-His-55 to glutamate. Both for HA-H55E and the double mutant HA-H55E/H93N transport activity at pH 6.0 was only 10% of wild type (HA-hPAT1: 272 ± 36 fmol/10 min per 400 000 cells; HA-H55E: 28 ± 1 fmol/10 min per 400 000 cells; HA-H55E/H93N: 26 ± 3 fmol/10 min per 400 000 cells) uptake and equally low as uptake into cells transfected with empty vector. We conclude that HA-hPAT1 behaves functionally exactly as hPAT1 does. His-55 seems to be essential for the transport function of hPAT1. His-135 is irrelevant. His-93 does not seem to be essential for H⁺ binding since mutation of this residue to asparagine does not abolish the transport function.

3.5. Protein expression of HA-hPAT1 and mutants

To evaluate whether the loss of transport function of certain HA-hPAT1 histidine mutants might be due to a decreased level of protein in the plasma membrane, Western blot analyses of biotinylated cell surface proteins were performed. In Fig. 5, immunoblot analyses of proteins isolated from the cell surface of non-transfected HRPE cells (NT) and HRPE cells transfected with empty vector pSPORT1 or the construct containing the HA-hPAT1 and the HA-hPAT1-histidine mutants cDNA are shown. For HA-hPAT1 and the non-transporting or less-transporting histidine mutants HA-H55A, HA-H55N, HA-H93A and HA-H93N, their prominent expression in the plasma membrane of HRPE cells is demonstrated. Signals for cytosolic β -tubulin III were detected in the total cell lysate but not in the cell surface protein fraction. We conclude that the loss of transport function in both His-55 mutants and in the HA-H93A mutant is not due to diminished protein expression. We confirmed this conclusion using a second independent approach, namely immunofluorescence analyses by confocal laser scanning microscopy. Cells transfected with the empty vector pSPORT1 or the construct containing the cDNA of HA-hPAT1 or histidine mutants were incubated with the primary rabbit anti-HA-Tag antibody followed

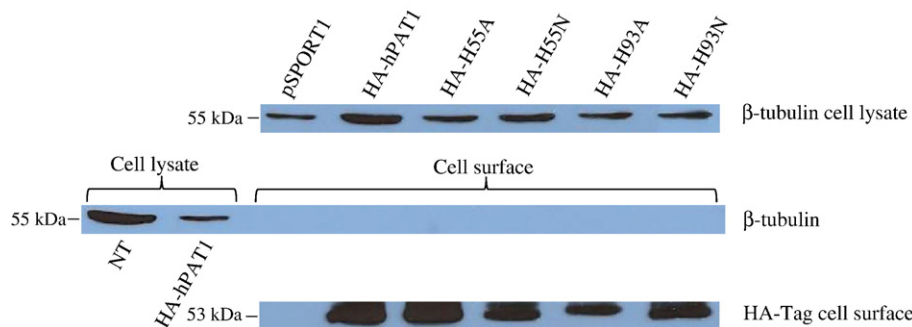


Fig. 5. Immunoblot analysis of HA-hPAT1 and histidine mutants expressed in HRPE cells. Proteins of non-transfected HRPE cells (NT) and HRPE cells transfected with empty vector pSPORT1 as control and HA-hPAT1, HA-H55A, HA-H55N, HA-H93A and HA-H93N cDNA were used for Western blot analysis. Total cell lysate and cell surface proteins, separated by SDS-PAGE, were transferred onto nitrocellulose membranes and probed with a rabbit monoclonal anti- β -tubulin III antibody. A rabbit monoclonal anti-HA-Tag antibody was used to detect proteins isolated by cell surface biotinylation. A horseradish peroxidase-conjugated anti-rabbit IgG antibody was used for labeling and blots were visualized by chemiluminescence on X-ray film.

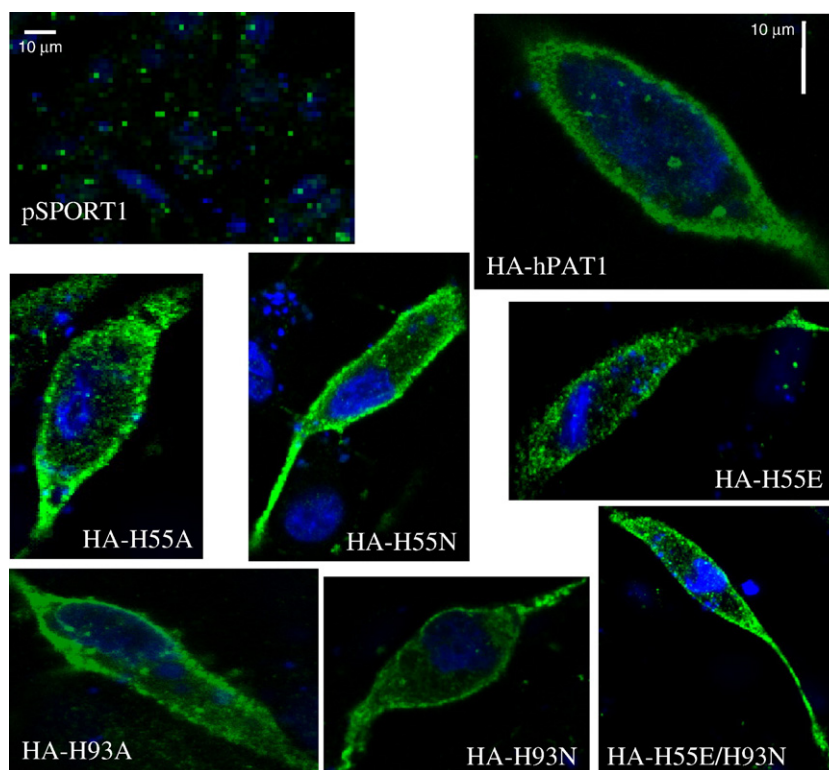


Fig. 6. Immunofluorescence localization of HA-hPAT1 and mutants in transfected HRPE cells using confocal laser scanning microscopy. Cells were transfected with either empty vector as control or the construct containing the HA-hPAT1 and the mutant proteins HA-H55A, HA-H55N, HA-H55E, HA-H93A, HA-H93N and HA-H55E/H93N cDNA, fixed, incubated with the primary rabbit anti-HA-Tag antibody and stained with a secondary anti-rabbit AlexaFluor®488 antibody. Nuclei were stained with DAPI.

by a secondary anti-rabbit AlexaFluor®488 antibody. Nuclei were stained with DAPI. As shown in Fig. 6, HA-hPAT1 and the mutant proteins HA-H55A, HA-H55N, HA-H55E, HA-H93A, HA-H93N and HA-H55E/H93N are localized in the plasma membranes. Intracellular staining was observed in addition to membrane labeling, which might be caused by the overexpression of HA-hPAT1 and mutant protein. HRPE cells transfected with empty vector pSPORT1 alone were analyzed for background-fluorescence. No labeled cell membranes were found.

3.6. Effects of DEPC on hPAT1 and HA-hPAT1 and mutants

To obtain further evidence for the role of specific histidine residues in H^+ binding, the sensitivity of hPAT1, HA-hPAT1 and mutants HA-H55A, HA-H93A and HA-H135A expressed in HRPE cells to DEPC was tested. We had demonstrated that DEPC-treatment strongly affects the affinity of hPAT1 for its substrates but this was done using Caco-2 cells [18]. In the present study, we first characterized the effect of DEPC on L-[3H]proline transport in hPAT1-HRPE cells. DEPC treatment (0.3 mM) inhibited proline uptake completely within 5 to 10 min (Fig. 7A). A 3 min treatment time was chosen for further experiments. From the dose–response relationship (Fig. 7B), an IC_{50} value of 0.13 ± 0.03 mM was estimated. The influence of DEPC on the K_t and V_{max} values of L-proline uptake into hPAT1-HRPE cells was determined in substrate saturation studies (Fig. 7C). The K_t value of L-proline uptake, determined by linear regression

of the data shown as Eadie–Hofstee plot, was 1.9 ± 0.3 mM in control cells and 4.3 ± 0.8 mM after DEPC treatment. The V_{max} values were not significantly different (8.2 ± 1.0 nmol/10 min per 400 000 cells in control cells and 7.6 ± 1.2 nmol/10 min per 400 000 cells after DEPC treatment, respectively). Hence, as it has been shown in Caco-2 cells expressing hPAT1 constitutively, treatment with DEPC at a concentration close to its IC_{50} value affected only the Michaelis constant of L-proline uptake via the cloned human PAT1. In the next series of experiments, the effect of DEPC treatment (10 min, 0.3 mM) on L-[3H]proline transport via HA-hPAT1 and histidine mutants was determined (Fig. 7D). DEPC did not affect transport in mutants where hPAT1 activity had been knocked out completely. In mutants HA-H93N and the mutants that transport L-[3H]proline comparable to wild type hPAT1, DEPC treatment reduced uptake by $>80\%$.

In conclusion, our results demonstrate that His-55 is obligatory for L-proline transport via hPAT1. Western blot and immunofluorescence analyses revealed that the loss of function is not due to lower protein expression or integration in the cell plasma membrane. This residue seems to be involved in binding and translocation of H^+ during the conformational change of the protein when transporting the substrate in a cotransport mode as it has been shown for His-57 in PEPT1 [14]. His-93 could play a role for a correct conformation of the protein in the membrane. Besides His-55 in rat, rabbit or mouse PAT1, other histidine residues might also be relevant (positions such as His-12, His-103, His-104, His-137, or His-248 in hPAT1). In

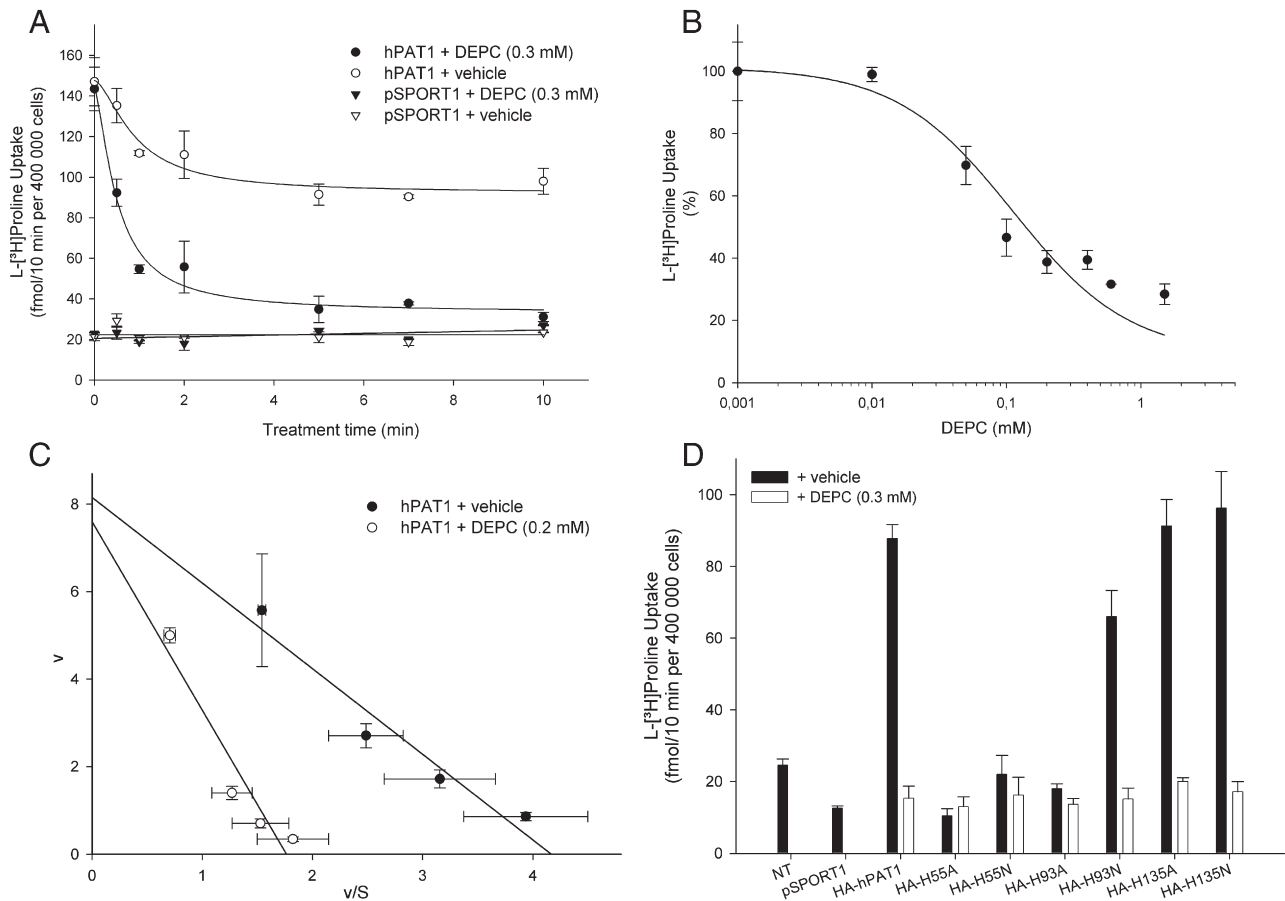


Fig. 7. Effect of DEPC on the transport function of hPAT1, HA-hPAT1 and mutants. A: HRPE cells expressing vector (pSPORT1) alone or hPAT1 were washed and then incubated with DEPC (0.3 mM) or ethanol as vehicle (0.2%) in buffer (pH 7.5) for 0 to 10 min at room temperature. After the incubation time indicated, cells were washed twice and incubated with uptake buffer pH 6.0 containing L-[³H]proline (20 nM) for 10 min. B: HRPE cells expressing hPAT1 were washed and incubated with DEPC at different concentrations. After 3 min, cells were washed twice and incubated with uptake buffer pH 6.0 containing L-[³H]proline (20 nM) for 10 min. C: hPAT1-HRPE cells treated for 3 min with 0.2 mM DEPC or vehicle (0.2% ethanol) were washed and incubated with buffer at pH 6.0 containing L-[³H]proline (20 nM) and increasing concentrations of unlabeled L-proline (0–10 mM) for 10 min. Uptake in vector-transfected cells was subtracted from uptake in hPAT1-transfected cells to calculate hPAT1-specific uptake. Results are given as Eadie–Hofstee plots. V: uptake of L-proline in nmol/10 min per 400 000 cells; S: L-proline concentration in mM. D: HRPE cells transfected with hPAT1, HA-hPAT1 or HA-H55A, HA-H55N, HA-H93A, HA-H93N, HA-H135A and HA-H135N cDNA were incubated for 10 min with DEPC (0.3 mM) or ethanol as vehicle (0.2%, control) in buffer pH 7.5 at room temperature. Uptake of L-[³H]proline (20 nM) was measured at pH 6.0 for 10 min. Data are means \pm S.E.M., $n=4$.

hPAT1, according to the 11 TMD model, His-55 is located near the intracellular surface of the first putative transmembrane domain. According to the 9 TMD model, His-55 would be located in the first cytoplasmatic loop [3]. Our data indirectly support the concept of the 11 TMD topology model.

This study represents the first mutational analysis of a member of the PAT-family. Because PAT1 accepts both glycine and L-proline as substrates and because the system is expressed in intestine and kidney, this transporter might play a key role in the human disease iminoglycinuria [23–25]. Hence, further mutational analyses and cell surface expression studies of hPAT1 proteins are imperative.

Acknowledgments

This work was supported by the State Saxony-Anhalt Life Sciences Excellence Initiative and by Deutsche Forschungsgemeinschaft grant BR 1317/4-2. We thank Ellen Closs, University of Mainz, for helpful discussions of surface biotinylation me-

thodology and Frank Erdmann and Matthias Weiwad, Max-Planck Research Unit Halle, for laser scanning microscopy. This work is part of the doctoral thesis of Linda Metzner.

References

- [1] C. Sagne, C. Agulhon, P. Ravassard, M. Darmon, M. Hamon, S. El Mestikawy, B. Gasnier, B. Giros, Identification and characterization of a lysosomal transporter for small neutral amino acids, *Proc. Natl. Acad. Sci. U. S. A.* 98 (2001) 7206–7211.
- [2] M. Boll, M. Foltz, I. Rubio-Aliaga, G. Kottra, H. Daniel, Functional characterization of two novel mammalian electrogenic proton-dependent amino acid cotransporters, *J. Biol. Chem.* 277 (2002) 22966–22973.
- [3] Z. Chen, Y.L. Fei, C.M. Anderson, K.A. Wake, S. Miyauchi, W. Huang, D.T. Thwaites, V. Ganapathy, Structure, function and immunolocalization of a proton-coupled amino acid transporter (hPAT1) in the human intestinal cell line Caco-2, *J. Physiol.* 546 (2003) 349–361.
- [4] D.T. Thwaites, G.T.A. McEwan, M.J. Cook, B.H. Hirst, N.L. Simmons, H⁺-coupled (Na⁺-independent) proline transport in human intestinal (Caco-2) epithelial cell monolayers, *FEBS Lett.* 333 (1993) 78–82.

- [5] G. Ranaldi, K. Islam, Y. Sambuy, D-cycloserine uses an active transport mechanism in the human intestinal cell line Caco 2, *Antimicrob. Agents Chemother.* 38 (1994) 1239–1245.
- [6] C.M.H. Anderson, D.S. Grenade, M. Boll, M. Foltz, K.A. Wake, D.J. Kennedy, L.K. Munck, S. Miyauchi, P.M. Tayler, F.C. Campbell, B.G. Munck, H. Daniel, V. Ganapathy, D.T. Thwaites, H⁺/Amino acid transporter 1 (PAT1) is the imino acid carrier: An intestinal nutrient/drug transporter in human and rat, *Gastroenterology* 127 (2004) 1410–1422.
- [7] L. Metzner, J. Kalbitz, M. Brandsch, Transport of pharmacologically active proline derivatives by the human proton-coupled amino acid transporter hPAT1, *J. Pharmacol. Exp. Ther.* 309 (2004) 28–35.
- [8] M. Brandsch, Transport of L-proline, L-proline-containing peptides and related drugs at mammalian epithelial cell membranes, *Amino Acids* 31 (2006) 119–136.
- [9] D.T. Thwaites, C.M. Anderson, Deciphering the mechanisms of intestinal imino (and amino) acid transport: the redemption of SLC36A1, *Biochim. Biophys. Acta* 1768 (2007) 179–197.
- [10] M. Foltz, M. Mertl, V. Dietz, M. Boll, G. Kottra, H. Daniel, Kinetics of bidirectional H⁺ and substrate transport by the proton-dependent amino acid symporter PAT1, *Biochem. J.* 386 (2005) 607–616.
- [11] D.T. Thwaites, C.M. Anderson, H⁺-coupled nutrient, micronutrient and drug transporters in the mammalian small intestine, *Exp. Physiol.* 92 (2007) 603–619.
- [12] E. Padan, L. Patel, H.R. Kaback, Effect of diethylpyrocarbonate on lactose/proton symport in *Escherichia coli* membrane vesicles, *Proc. Natl. Acad. Sci.* 76 (1979) 6221–6225.
- [13] M. Brandsch, C. Brandsch, M.E. Ganapathy, C.S. Chew, V. Ganapathy, F.H. Leibach, Influence of proton and essential histidyl residues on the transport kinetics of the H⁺/peptide cotransport systems in intestine (PEPT 1) and kidney (PEPT 2), *Biochim. Biophys. Acta* 1324 (1997) 251–262.
- [14] Y.-J. Fei, W. Liu, P.D. Prasad, R. Kekuda, T.G. Oblak, V. Ganapathy, F.H. Leibach, Identification of the histidyl residue obligatory for the catalytic affinity of the human H⁺/peptide cotransporters PEPT1 and PEPT2, *Biochemistry* 39 (1997) 452–460.
- [15] H.M. Said, R. Mohammadkhani, Folate transport in intestinal brush border membrane: involvement of essential histidine residue(s), *Biochem. J.* 290 (1993) 237–240.
- [16] T.L. Trosper, K.D. Philipson, Functional characteristics of the cardiac sarcolemmal monocarboxylate transporter, *J. Membr. Biol.* 112 (1989) 15–23.
- [17] B. Rahman, H.P. Schneider, A. Bröer, J.W. Deitmer, S. Bröer, Helix 8 and helix 10 are involved in substrate recognition in the rat monocarboxylate transporter MCT1, *Biochemistry* 38 (1999) 11577–11584.
- [18] L. Metzner, M. Brandsch, Influence of a proton gradient on the transport kinetics of the H⁺/amino acid cotransporter PAT1 in Caco-2 cells, *Eur. J. Pharm. Biopharm.* 63 (2006) 360–364.
- [19] M. Boll, M. Foltz, I. Rubio-Aliaga, H. Daniel, A cluster of proton/amino acid transporter genes in the human and mouse genomes, *Genomics* 82 (2003) 47–56.
- [20] R.D. Blakely, J.A. Clark, G. Rudnick, S.G. Amara, Vaccinia-T7 RNA polymerase expression system: evaluation for the expression cloning of plasma membrane transporters, *Anal. Biochem.* 194 (1991) 302–308.
- [21] C. Staib, I. Drexler, G. Sutter, Construction and isolation of recombinant MVA, *Methods Mol. Biol.* 269 (2004) 77–100.
- [22] L. Metzner, G. Kottra, K. Neubert, H. Daniel, M. Brandsch, Serotonin, L-tryptophan and tryptamine are effective inhibitors of the human amino acid transport system PAT1, *FASEB J.* 19 (2005) 1468–1473.
- [23] M. Boll, H. Daniel, B. Gasnier, The SLC36 family: proton-coupled transporters for the absorption of selected amino acids from extracellular and intracellular proteolysis, *Pflügers Arch.* 447 (2004) 776–779.
- [24] A. Bröer, J.A. Cavanaugh, J.E. Rasko, S. Bröer, The molecular basis of neutral aminoacidurias, *Pflügers Arch.* 451 (2006) 511–517.
- [25] S. Miyauchi, E.L. Abbot, L. Zhuang, R. Subramanian, V. Ganapathy, D.T. Thwaites, Isolation and function of the amino acid transporter PAT1 (slc36a1) from rabbit and discrimination between transport via PAT1 and system IMINO in renal brush-border membrane vesicles, *Mol. Membr. Biol.* 22 (2005) 549–559.